Artificial Intelligence Assisted Residual Strength and Life Prediction of Fiber Reinforced Polymer Composites

Partha Pratim Das[1]
The University of Texas at Arlington, Arlington, TX, USA 76019

Muthu Elenchezhian[2]
Purdue University, West Lafayette, IN USA 47906

Vamsee Vadlamudi[3] and Rassel Raihan.[4]
The University of Texas at Arlington, Arlington, TX, USA 76019

Institute of Predictive Performance Methodologies, UTA Research Institute, Fort Worth, TX

With the increased use of composite materials, researchers have developed many approaches for structural and prognostic health monitoring. Broadband Dielectric Spectroscopy (BbDS)/Impedance Spectroscopy (IS) is a state-of-the-art technology that can be used to identify and monitor the minute changes in damage initiation, accumulation, interactions, and the degree of damage in a composite under static and dynamic loading. This work presents a novel artificial neural network (ANN) framework for fiber-reinforced polymer (FRP) composites under fatigue loading, which incorporates dielectric state variables to predict the life (durability) and residual strength (damage tolerance) from real-time acquired dielectric permittivity of the material. The findings of this study indicate that this robust ANN-based prognostic framework can be implemented in FRP composite structures, thereby assisting in preventing unforeseeable failure.

I. Introduction

Fiber-reinforced polymer (FRP) composite structures are a complex system of materials that have been implemented extensively in aviation and marine sectors and consumer-level products, sports goods, and medical equipment. Although they are lightweight yet strength-wise comparable to traditional metal components, FRP composites exhibit vulnerability in terms of the unpredictable nature of damage generation, progression, and ultimate failure. Dynamic loading (i.e., fatigue, etc.) is a critical loading case for a composite structure that promotes different stages of damage initiation and propagation during its service life. Reifsnider et al. observed that though initiation and damage development are progressive in nature in the composites, it can trigger a sudden death phenomenon which, if undetected, can be catastrophic and irreversible (Fig. 1) [1]. As observed in Fig. 1, matrix cracks are the firsts to initiate at different locations until they reach a saturated state when fiber-matrix debonding and delaminations come into perspective. This saturation state is defined as a Characteristic Damage State (CDS) that is a precursor for severe damage. As a composite reaches CDS, its stiffness drops though it retains strength [2]. In laboratory-based research, the global and local stiffness degradation at CDS can be identified from state-of-the-art mechanical characterization

[1] PhD Student, Mechanical and Aerospace Engineering, AIAA Member.
[2] Postdoctoral Researcher, School of Aeronautics and Astronautics, AIAA member.
[3] Research Scientist II, UTA Research Institute, AIAA Member.
[4] Assistant Professor, Mechanical and Aerospace Engineering.

techniques (i.e., destructive fatigue test of coupons, strain measurement using digital image correlation, fiber optics sensors, extensometers, and strain gauges). However, in real-life structures, identifying damage states requires incorporating external or internal sensors to monitor the structural health in situ non-destructively.

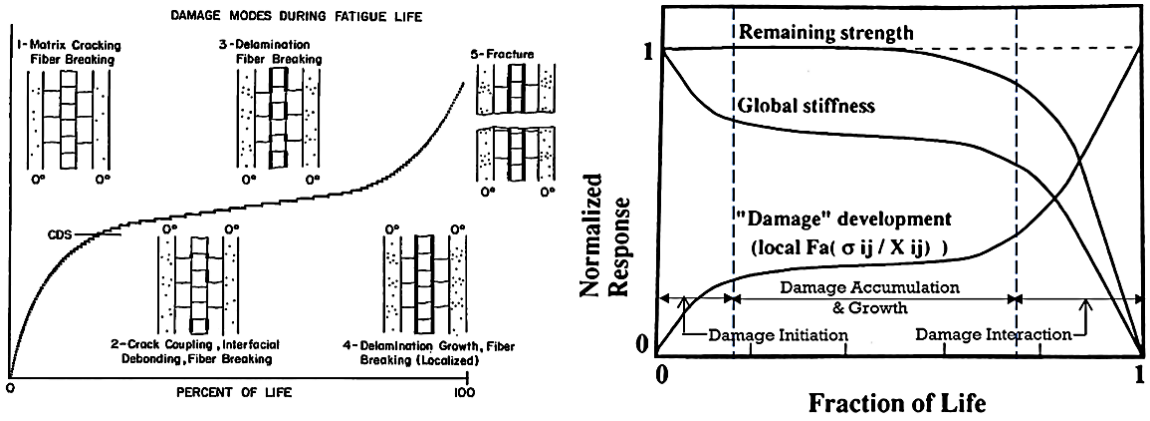

Fig. 1 Damage progression in composites and relation of remaining strength, global stiffness with life [3]

Because of the rising complexity and demand for high reliability and efficiency of composite parts, traditional maintenance approaches for assessing material state are becoming obsolete. Given the unpredictable nature of damage progression in composites, artificial intelligence (AI) based predictive models can be trained to identify the damage precursors from extensive sensor data throughout the service life of a composite [4]. Over the past few decades, different AI models have been developed and trained for composite diagnostics and prognostics, including but not limited to linear and multivariate regression models [5,6], support vector machine [7,8], tree-based methods [9,10], unsupervised clustering algorithms [11–14], hybrid models [15,16]. However, with the advancement of artificial neural network (ANN) based algorithms, modeling damage and prognostics have been more efficient and accurate [17–20]. In a recent publication, Elenchezian et al. presented a comprehensive literature review of the ANN models developed over the past few decades in structural health monitoring and prognostic health management of FRP composites [21].

This work presents a novel ANN-based prediction framework, which incorporates acquired in-situ dielectric data from Dielectric Spectroscopy (DS) to predict the life and residual strength (RS) of polymer composites under fatigue loading. DS is a material characterization technique simulating a parallel plate capacitor setup where the sample is considered the dielectric material. An alpha analyzer employs an AC voltage across the sample, and dielectric properties are analyzed from the measured impedance. Dielectric state variables (i.e., real permittivity, etc.), the direct indicators of damage development during fatigue, are effectively utilized as the in-situ rate of change of these state variables can be correlated with the rate of damage interaction and stiffness degradation at a specific time [22]. In this study, Fiber optic sensors (FOS) have been used to monitor stiffness degradation during fatigue. FOS based on Fiber Bragg Gratings (FBGs) is a state-of-the-art strain sensing technology that can be multiplexed and installed in composite parts to achieve a quasi-distributed strain measurement. This prediction framework consists of two coupled ANN-based multilayer perceptron (MLP) models. The first developed model predicts the life of the composite solely from in situ dielectric permittivity data, and the output is passed through a second developed model that can predict the RS of the composite part with high accuracy. This paper comprehensively outlines the proposed framework and reports the relevant prediction accuracies.

II. Experimentation

A. Test Material Preparation

In this study, composite laminates were fabricated using unidirectional epoxy-impregnated E-glass fiber prepregs. Each laminate consisted of 8 plies with stacking sequence $[-45°/0°/+45°/90°]_s$ to make a quasi-isotropic laminate. The manufacturing was done using the out-of-autoclave process in a Despatch composite curing oven. The laminate was cured at 135° C. Protomax water jet cutter was used to prepare the specimens in 254 mm × 38.1 mm as per the ASTM D3479 standard [23]. The specimens had an average thickness of 2 mm.

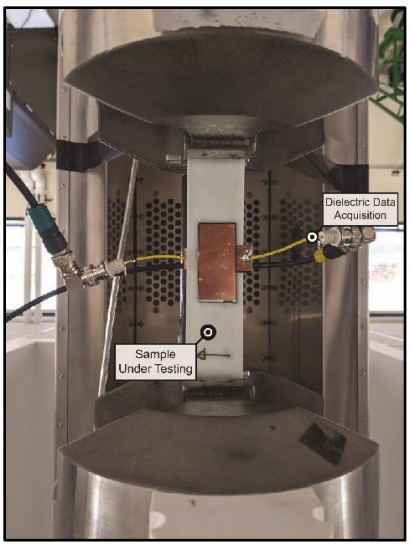

Fig. 2 Experimental setup for fatigue and residual strength tests with dielectric data acquisition

B. Experimental Design and Proposed Framework

Initially, randomly selected specimens were subjected to quasi-static tensile loading to determine the sample batch's mean ultimate tensile strength (UTS) as per ASTM D3039 [24]. The tests were carried out at a rate of 0.03 mm/s. Once the mean UTS was determined from the tests, Weibull analysis was utilized to obtain the 95% confidence levels, as shown in Table 1. From the mean UTS and mean cross-sectional area (73.25 mm^2), the mean breaking load was calculated to be 23 KN. This initially acquired data is used to design the tension-tension fatigue experiments for different mean stress levels (25%, 50%, and 75% of UTS), as described in Table 2. Then, initial fatigue tests were performed to determine respective 95% confidence intervals for each mean stress level (Table 3). The frequency of the tests has been predefined as 2 Hz.

Table 1: Results of quasi-static tensile tests

Mean Ultimate Tensile Strength (MPa)	Scale Parameter (MPa)	Shape Parameter	95 % Confidence Limit – Lower (MPa)	95% Confidence Limit – Upper (MPa)
314.12	323.54	16.37	314.71	332.62

Table 2: Fatigue test parameters

Mean Stress %	Mean Stress (MPa)	Max Stress (MPa)	Min Stress (MPa)	R ratio
75 %	235.58	298.41	172.76	0.578
50 %	157.06	219.88	94.23	0.428
25 %	78.53	141.35	15.70	0.111

Table 3: Weibull analysis of initial fatigue test results

Mean Stress % Condition	Shape Parameter	Mean Cycles to Failure – Scale Parameter	95 % Confidence Limit – Lower	95% Confidence Limit – Upper
75 %	1.7392	764.70	500.51	1168.34
50 %	2.6236	60504.49	49756.22	73574.57
25 %	4.2211	456882.75	390979.68	533894.37

Secant Stiffness and dielectric permittivity data, considered state variables in this work, were captured utilizing embedded fiber optics and dielectric spectroscopy sensors. Fig. 2 shows the experimental setup for one test with dielectric data acquisition using extremely conductive silver epoxy adhesive and copper electrodes. Secant stiffness and dielectric permittivity data were then normalized to their initial values at the end of the quasi-static ramp up phase. The fatigue life was also normalized to the number of cycles to failure. Hence a unit value indicates the failure of the individual specimen. The first and second derivatives of these normalized parameters' curves were acquired from a

5th-order polynomial fit of the respective entities. In this case, the first-order derivative displays the instantaneous rate of change, and the second-order derivative explains the acceleration of the individual parameters' changes.

For the life prediction model, fatigue tests were carried out up to failure for each mean stress level. However, for residual strength prediction, a training dataset has been generated from fatigue tests for 50% mean stress level, which was done up to predefined cycle counts (less than 95% lower confidence 49756 ~ 50000 cycles). Once the predefined fatigue test is completed, the specimen is unloaded to zero load, and a quasi-static tensile test is done to obtain the residual strength. For all the fatigue tests, in situ dielectric permittivity data at 100 Hz frequency was acquired with the Novocontrol Broadband Dielectric Spectrometer. Then, two Artificial Neural Network (ANN) models were developed and coupled from the acquired data to form a framework that incorporates these parametric changes and predicts the life and residual strength of the specimens before the failure occurs. In summary, the proposed prediction framework is shown in Fig. 3.

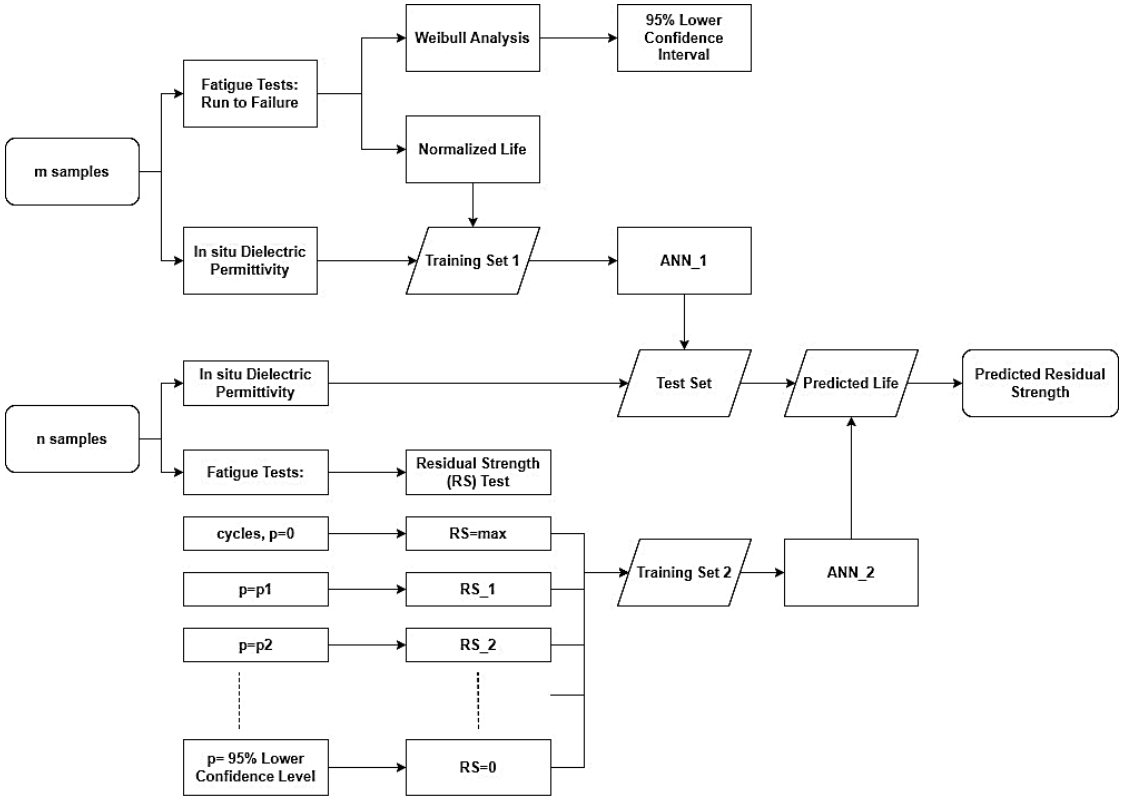

Fig. 3 Proposed framework to predict life and residual strength

III. Model Development and Analysis

A. Initial Fatigue Results

Fatigue experiments have been carried out for the samples in force control mode. After a predefined number of cycles is reached for fatigue, a residual strength test is carried out. Fig. 4a shows the input axial force response over time for a fatigue test run up to 5000 cycles. Fig. 4b shows the output strain response for the sample. From the strain response in Fig. 4b, it is evident that stiffness degrades over time in fatigue. The phenomenon can be attributed to the damage development during fatigue that decreases inter-molecular attraction and creates free volume and interfaces in the material.

Consequently, the dielectric response for the test is shown in Fig. 5. It can be seen that the dielectric response correlates with the strain response. During the fatigue phase of the test, the dielectric permittivity value has an accelerated ramp-down at the beginning that continues at a steady pace similar to stiffness evolution. In the residual strength test phase, the dielectric permittivity value decreases as well, but at a higher rate than in the fatigue phase. This phenomenon can be attributed to the increased number of damage interactions of the damage modes developed during the fatigue phase.

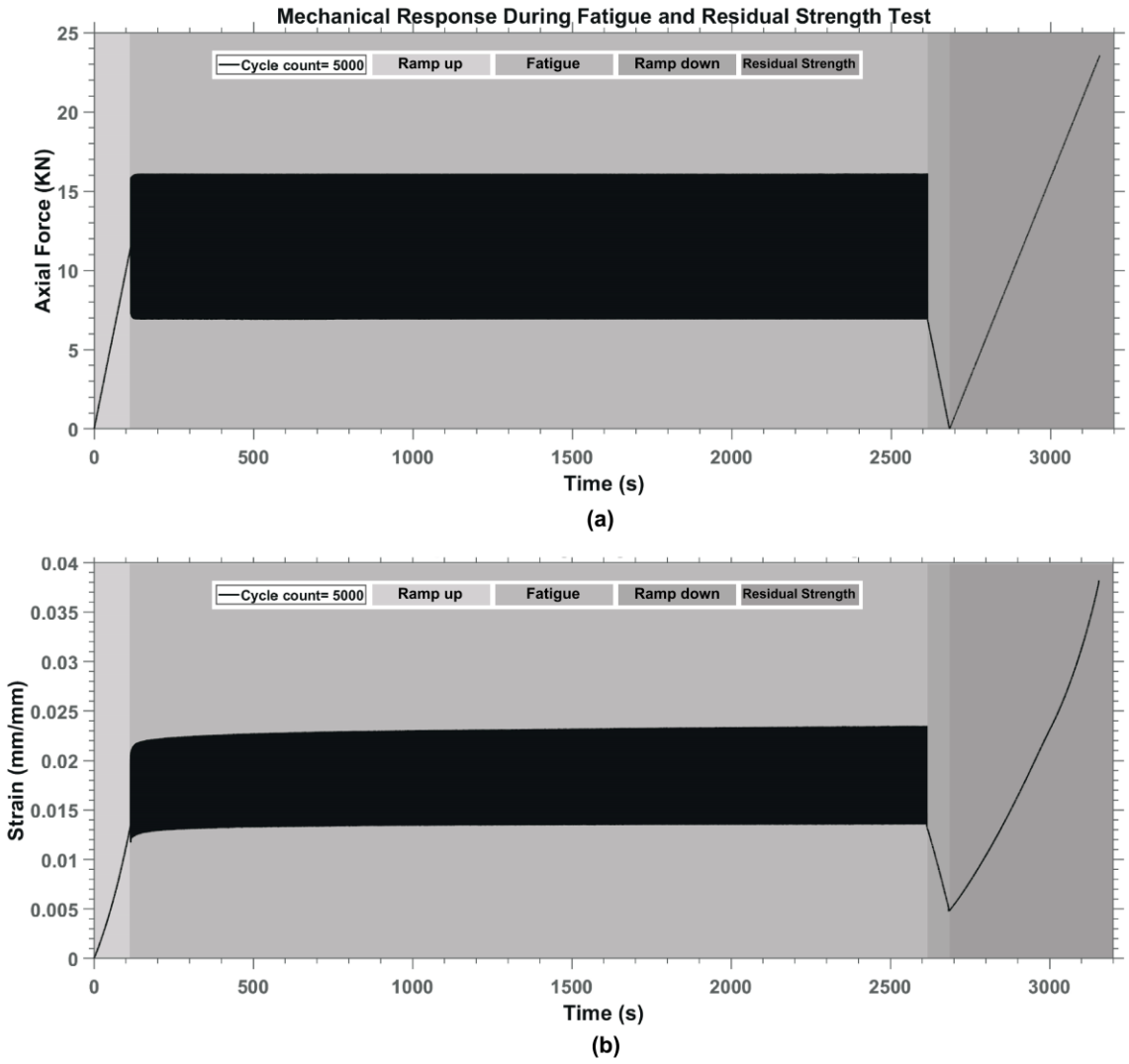

Fig. 4 Mechanical response during fatigue and residual strength test; a) force response, b) strain response

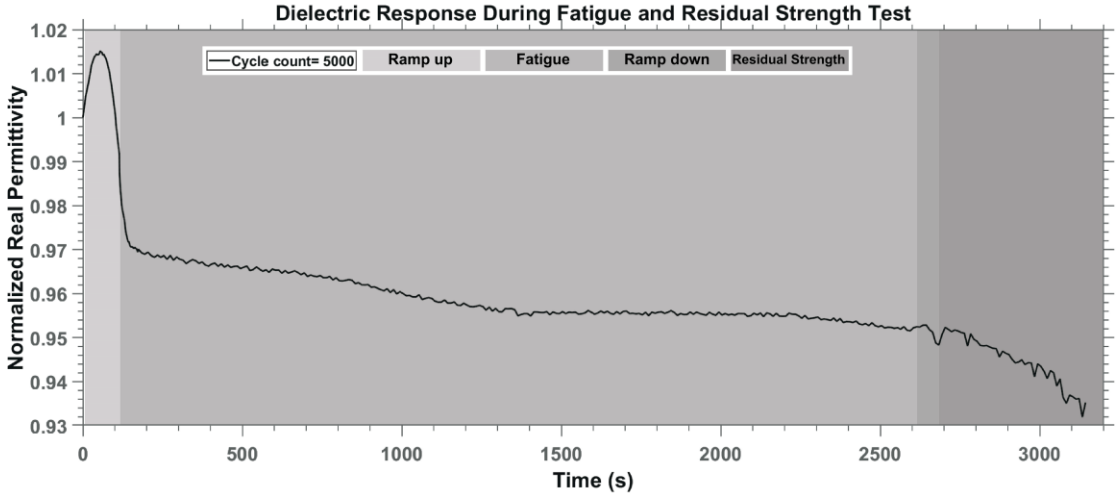

Fig. 5 Dielectric response during fatigue and residual strength test

B. Analysis of State Variables

Figure 6 represents the mechanical (stiffness), and dielectric (permittivity) response during the fatigue loading of a specimen tested at 50% mean stress level up to failure. The stiffness vs. life curve (normalized) is similar to observations made in the literature (Fig. 1), except for a few artifacts. A sharp decrease in the beginning and end of the fatigue is notable, primarily due to the 50% mean stress level. At this stress level, and considering the amplitude of fatigue loading, the material would have attained the CDS (Characteristic Damage State), resulting in this initial sharp decrease in stiffness, unlike the behavior in Fig. 1. From Fig. 6, it is also evident that there is an accelerated decrease in the permittivity starting at about 75% of the life, which can serve as a precursor for indicating the beginning of the material's end of life.

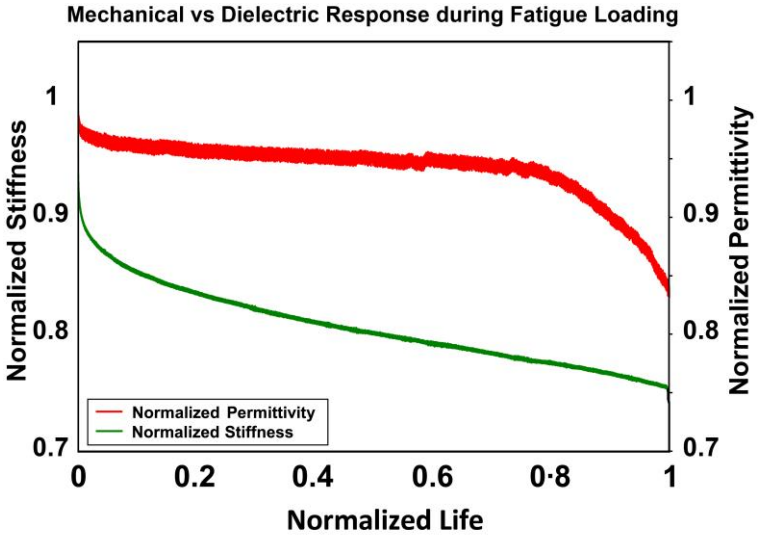

Fig. 6 Stiffness and permittivity response over normalized life during fatigue

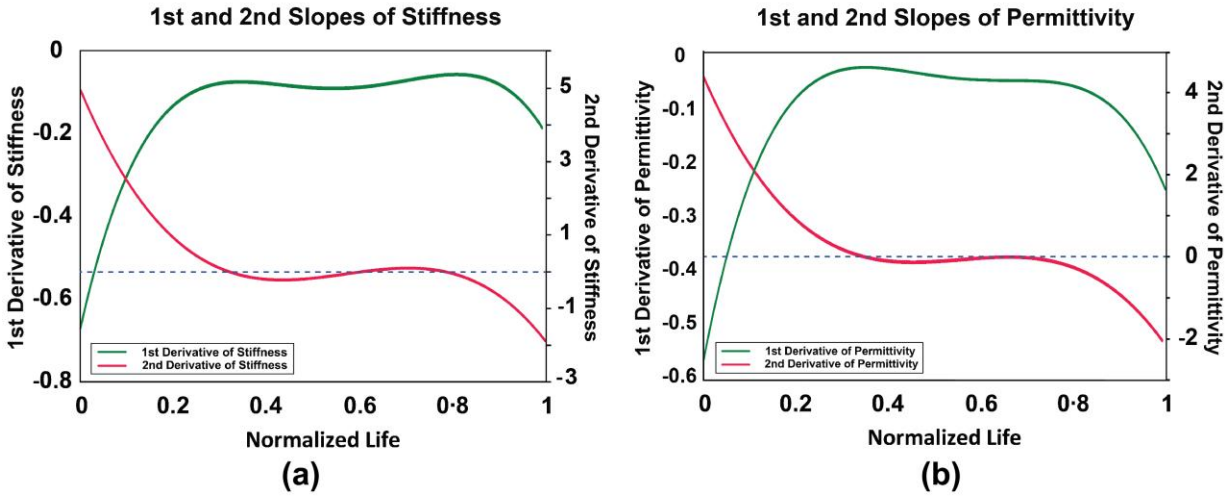

Fig. 7 1st and 2nd derivatives of a) stiffness and b) permittivity over normalized life

Figure 7 represents the derivatives for the representative state variables. As described before, the first derivative represents the rate of a property change, whereas the second derivate represents the acceleration of the change. The representative acceleration of stiffness and permittivity are normalized concerning their maximum values and compared, as shown in Fig. 8. It can be observed that the acceleration of mechanical and dielectric state variables follows a similar trend until about 50% of life. For both stiffness and permittivity values, the magnitude of the acceleration is higher in the beginning and starts to decrease gradually, leading to a saturation phase. However, the

second inflection point in the acceleration curves shows that the magnitude of acceleration in the dielectric response increases earlier than the mechanical response. Here, permittivity acceleration starts to increase around 70% of life. In contrast, stiffness acceleration starts to increase after 75% of life. Thus, the dielectric response provides an earlier warning of the beginning of the failure of the material. This second point of inflection served as the basis for determining the percentage of life and, consequently, the number of cycles at that instance. For instance, the average life percentage and number of cycles are 68.78% and 53655, respectively, based on permittivity, at which the failure is imminent for this laminate under the given loading conditions. However, based on the second point of inflection calculated from stiffness, the average life percentage and number of cycles are 71.74% and 59669, respectively.

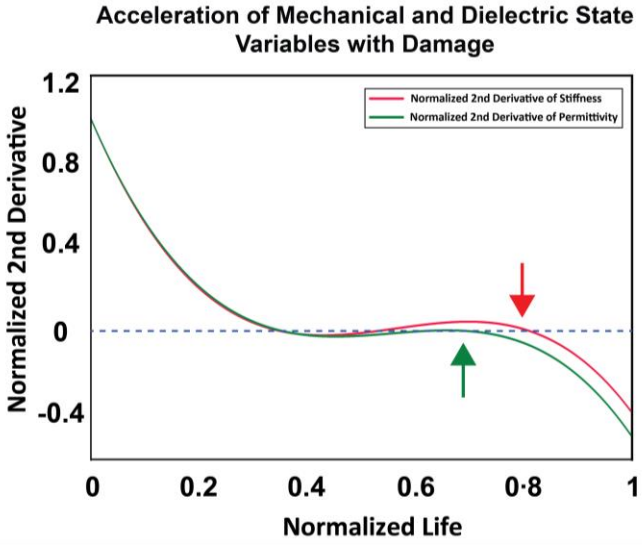

Fig. 8 Comparison of the 2nd derivatives of stiffness and permittivity throughout life

Figure 9 shows how the acceleration of the permittivity changes for the three different loading conditions. It can be observed that, for all three different loading conditions, the inflection point is identified at about 75-80% of the material's life, indicating the beginning of the end of failure of the composite specimen.

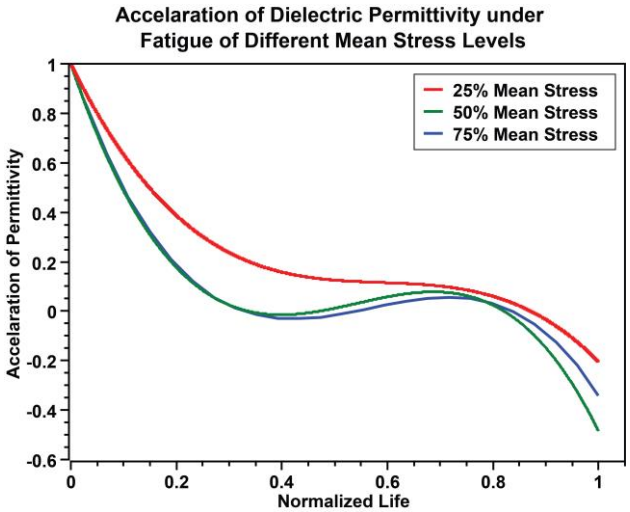

Fig. 9 Acceleration of permittivity throughout the life of the composite

C. ANN Analysis for Life Prediction

Until now, we discussed the physics-based approach of using real permittivity value and the stiffness value over life. This section explains the development of an AI algorithm using the in situ real permittivity data for each specimen, obtained over time, estimating the life at that instant and predicting the future.

At first, the input normalized real permittivity, and life data were converted to finite time steps of data to develop the MLP regression model for life prediction. The developed neural network architecture consists of three hidden layers and an output layer of 500 nodes. The grid search cross-validation method was adopted with a 5-fold cross-validation technique to find the optimal hyperparameters for the model. This method searched for the best mean R^2 score for a combination of different hyperparameters. The optimal hyperparameters for the developed model are presented in Table 4. This model is named "ANN_1" in this paper hereafter for convenience.

Table 4: Tuned hyperparameters for the life prediction model (ANN_1)

Hidden Layer Sizes	Activation Function	Solver	Learning Rate	Maximum Iterations
900, 200, 800	Rectified Linear Unit (ReLU) [25]	Adam [26]	0.0001	5000

This model's test data comprises 12 specimens tested up to different cycles below the 95% confidence level of cycles to fail for 50% mean stress level (i.e., 50000 cycles depicting whole fatigue life). For example, a fatigue test is carried out for a specimen up to 10000 cycles, and in situ dielectric data is recorded and converted to a vector of dielectric permittivity data at scaled timesteps (i.e., 100 timesteps ~ 10000 cycles or 0.20 normalized life). The remaining unknown dielectric permittivity values for the rest of the timesteps (i.e., 101 to 500 timesteps ~ 10001 to 50000 cycles or 0.2 to 1.0 normalized life) are then padded by zero (0) to make it interpretable for the model. Then the curated permittivity vector is provided to the developed model as a test observation to predict the specimen's life at the current state (i.e., 10000 cycles or 100th timestep) and future timesteps (i.e., any cycle counts greater than 10000 cycles or 101 to rest of the timesteps). This way, the output prediction curves were obtained from the ANN model for each test specimen, and a visual representation of the same is provided in Fig. 10.

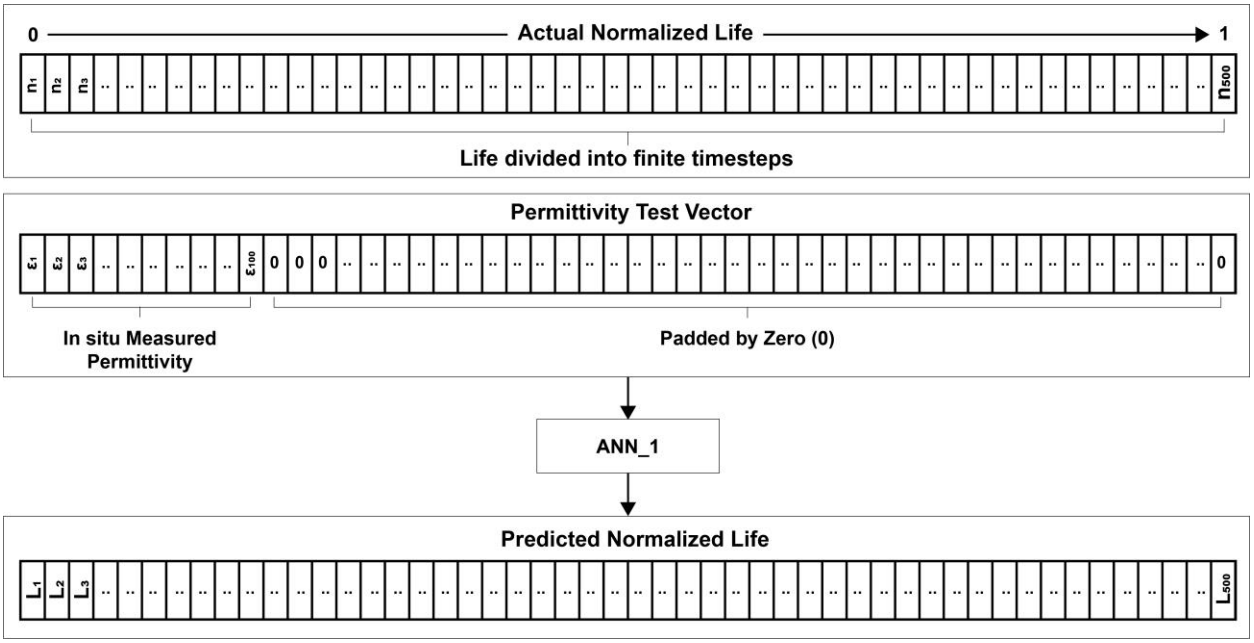

Fig. 10 Data curation methodology for model development and testing

Figure 11 shows the life prediction for 6 test specimens under fatigue for different predefined cycles compared with actual data. The average R^2 value for the 12 test specimens is 0.9326. It can be seen that the model does not perform very well for lower cycle dielectric permittivity inputs (i.e., for 10000 cycles where only the first 100 timestep data were input). However, as more dielectric data is available, the model performs well in predicting fatigue life.

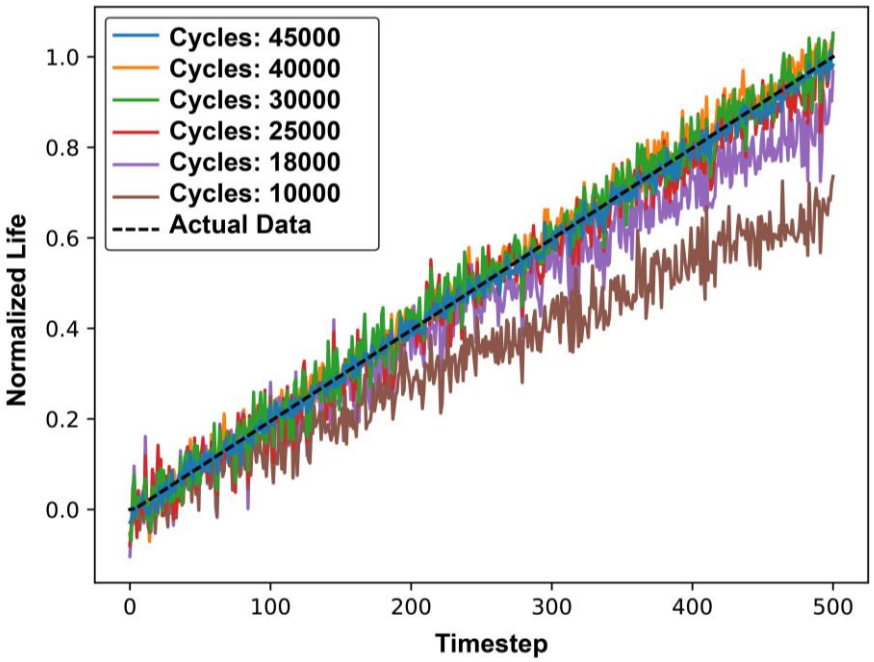

Fig. 11 Prediction of life from in-situ dielectric data using ANN_1

D. ANN Framework for Residual Strength Prediction

Fatigue generates damage in the composite structure, but if it doesn't fail, it can still withhold some strength, defined as the residual strength. A composite under service may face different loads that can generate damage inside. So, monitoring residual strength is of utmost importance. This work proposes a novel framework that can predict the residual strength of a composite part damaged due to fatigue. In this study, the proposed framework has coupled two ANNs together. The first model is the one that has already been described in the previous section. Specimens were tested in fatigue for different cycles, and their dielectric permittivity changes were recorded in situ. Then the residual strengths of the specimens were obtained using a quasi-static tensile test. From this, a new dataset is formed where input data consists of the normalized life, and the output data consists of the residual strength of the individual specimen. Fig. 12 shows the training dataset for this ANN model comprising normalized life as input and residual strength as output.

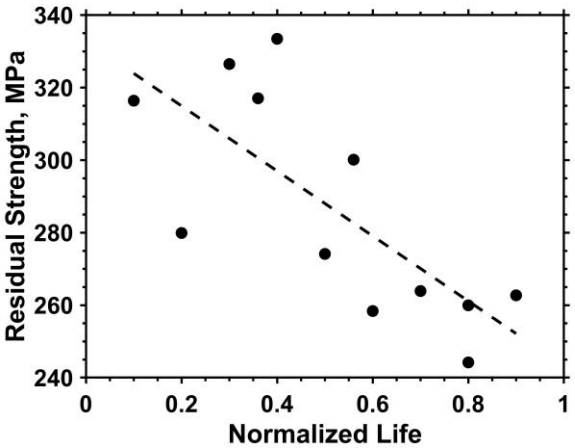

Fig. 12 Training dataset for ANN_2

An MLP regression model comprising three hidden layers and one output layer with a single node is generated from this training dataset. The hyperparameters of this model are tuned using grid search cross-validation and 5-fold

cross-validation techniques. Table 5 includes the optimal hyperparameters for the model to have the best mean R^2 score in the training set. This model is named "ANN_2" in this paper hereafter for convenience.

Table 5: Tuned hyperparameters for the residual strength prediction model (ANN_2)

Hidden Layer Sizes	Activation Function	Solver	Learning Rate	Maximum Iterations
58,30,77	Rectified Linear Unit (ReLU) [25]	LBFGS [27]	0.00011	5000

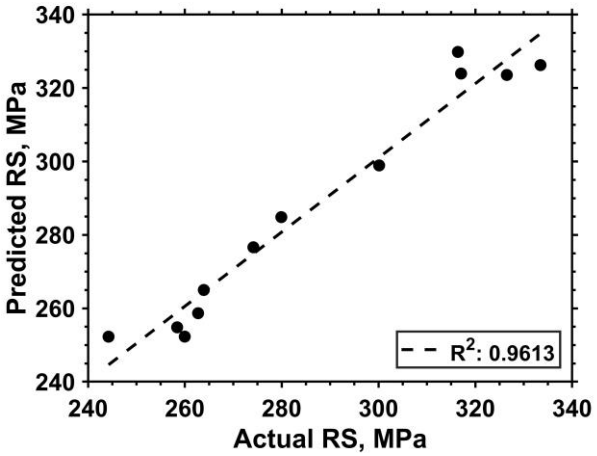

Fig. 13 Performance of residual strength prediction framework

In this study, the proposed framework couples ANN_1 and ANN_2 for residual life prediction. As a first step, the measured real permittivity data was passed through the ANN_1 model to estimate a specimen's current life at limited cycle fatigue. The output estimated life is then passed through the ANN_2 model, and the model predicts the residual life of the specimen. In total, 12 specimens under different cycle count fatigue were tested in this framework. Fig. 13 compares the actual residual strength and the predicted residual strength of the test specimens. The framework works reasonably well in residual strength prediction, as shown in Fig. 13, with an R^2 value of 0.9613. To summarize, this residual strength framework can be used to determine the present residual strength of a fatigue specimen based on the material's in situ dielectric permittivity response.

IV.Conclusion

This study presents a novel framework for prognostics utilizing artificial neural network algorithms. The framework can predict the current and future life and residual strength from in situ dielectric response of polymer composites during fatigue. Under fatigue loading, a composite part can develop progressive damage inside, leading to sudden, unavoidable failure under continued service conditions. The initiation and propagation of the damage can be correlated with the dielectric permittivity changes as they can interact with the morphological changes in materials. In this study, Dielectric Spectroscopy (DS) has been used to measure the permittivity values at 100 Hz during fatigue loading. Here, Two ANN-based multilayer perceptron models (namely life prediction model or ANN_1 and residual strength prediction model or ANN_2) have been developed and coupled. The first model is trained from dielectric and life data of specimens tested in fatigue up to failure. The second model is trained from the current life, and residual strength data for specimens tested in fatigue for different cycle counts. Then the life and residual strength of the test specimens were predicted from the proposed framework. The following conclusions can be drawn from this study:

- During fatigue, the material's stiffness degrades, which has a similar rate and acceleration of change as the dielectric permittivity, as both of these variables evolve due to damage growth and interactions. However, dielectric permittivity can predict the beginning of the end of life earlier than the stiffness degradation model.
- The life prediction model can predict the current life and future life span from dielectric permittivity with reasonable accuracy (average R^2 value of 0.9326 in the test dataset).

- The residual strength prediction framework can predict the residual strength of a specimen with an R^2 value of 0.9613. The framework takes in situ dielectric permittivity response and predicts current life using the life prediction model, followed by residual strength prediction from the residual strength prediction model.

To conclude, the proposed method can obtain good accuracies in predicting a composite part's life and residual strength from in situ dielectric response of the material under fatigue loading. However, the method includes different statistical data curation techniques, which need to be optimized. The investigated dataset is comparatively small; hence a much more comprehensive model developed with big data would be more effective, which is a scope of future study. Also, these shallow neural networks' computational times are not satisfactory. So, as a scope of future work, deep neural network-based sophisticated algorithms, such as recurrent neural networks (RNN), can be developed with big data to address these issues and move a step forward in composite prognostics health monitoring.

Acknowledgments

The authors would like to acknowledge and thank the scholars and the staff at the Institute for Predictive Performance Methodologies at the University of Texas at Arlington Research Institute for their tremendous support of this research work.

References

[1] Reifsnider, K. L., Henneke, E. G., Stinchcomb, W. W., and Duke, J. C. "DAMAGE MECHANICS AND NDE OF COMPOSITE LAMINATES." 1983, pp. 399–420. https://doi.org/10.1016/B978-0-08-029384-4.50032-8.

[2] Vadlamudi, V., Shaik, R., Raihan, R., Reifsnider, K., and Iarve, E. "Identification of Current Material State in Composites Using a Dielectric State Variable." *Composites Part A: Applied Science and Manufacturing*, Vol. 124, 2019, p. 105494. https://doi.org/10.1016/J.COMPOSITESA.2019.105494.

[3] Raihan, R., Adkins, J.-M., Baker, J., Rabbi, F., and Reifsnider, K. *Relationship of Dielectric Property Change to Composite Material State Degradation*. 2014.

[4] Chen, C. T., and Gu, G. X. "Machine Learning for Composite Materials." *MRS Communications*, Vol. 9, No. 2, 2019, pp. 556–566. https://doi.org/10.1557/MRC.2019.32.

[5] Tiryaki, S., and Aydin, A. "An Artificial Neural Network Model for Predicting Compression Strength of Heat Treated Woods and Comparison with a Multiple Linear Regression Model." *Construction and Building Materials*, Vol. 62, 2014, pp. 102–108. https://doi.org/10.1016/J.CONBUILDMAT.2014.03.041.

[6] Tsao, C. C., and Hocheng, H. "Taguchi Analysis of Delamination Associated with Various Drill Bits in Drilling of Composite Material." *International Journal of Machine Tools and Manufacture*, Vol. 44, No. 10, 2004, pp. 1085–1090. https://doi.org/10.1016/J.IJMACHTOOLS.2004.02.019.

[7] Das, S., Chattopadhyay, A., and Srivastava, A. N. "Classifying Induced Damage in Composite Plates Using One-Class Support Vector Machines." *AIAA journal*, Vol. 48, No. 4, 2010, pp. 705–718. https://doi.org/10.2514/1.37282.

[8] Sheng, W., Liu, Y., and Söffker, D. "A Novel Adaptive Boosting Algorithm with Distance-Based Weighted Least Square Support Vector Machine and Filter Factor for Carbon Fiber Reinforced Polymer Multi-Damage Classification." *Structural Health Monitoring*, Vol. 0, No. 0, 2022, pp. 1–17. https://doi.org/10.1177/14759217221098173/ASSET/IMAGES/LARGE/10.1177_14759217221098173-FIG9.JPEG.

[9] Liu, H., Liu, S., Liu, Z., Mrad, N., and Dong, H. "Prognostics of Damage Growth in Composite Materials Using Machine Learning Techniques." *Proceedings of the IEEE International Conference on Industrial Technology*, 2017, pp. 1042–1047. https://doi.org/10.1109/ICIT.2017.7915505.

[10] Das, P. P., Rabby, M. M., Vadlamudi, V., and Raihan, R. "Moisture Content Prediction in Polymer Composites Using Machine Learning Techniques." *Polymers*, Vol. 14, No. 20, 2022, p. 4403. https://doi.org/10.3390/polym14204403.

[11] Elenchezhian, M. R. P., Vadlamudi, V., Raihan, R., and Reifsnider, K. "Unsupervised Learning Methods for Identification of Defects in Heterogeneous Materials." *Proceedings of the American Society for Composites - 35th Technical Conference, ASC 2020*, 2020, pp. 839–850. https://doi.org/10.12783/ASC35/34900.

[12] Tang, J., Soua, S., Mares, C., and Gan, T. H. "A Pattern Recognition Approach to Acoustic Emission Data Originating from Fatigue of Wind Turbine Blades." *Sensors 2017, Vol. 17, Page 2507*, Vol. 17, No. 11, 2017, p. 2507. https://doi.org/10.3390/S17112507.

[13] Sawan, H. A., Walter, M. E., and Marquette, B. "Unsupervised Learning for Classification of Acoustic Emission Events from Tensile and Bending Experiments with Open-Hole Carbon Fiber Composite Samples." *Composites Science and Technology*, Vol. 107, 2015, pp. 89–97. https://doi.org/10.1016/J.COMPSCITECH.2014.12.003.

[14] Sierra-Pérez, J., Güemes, A., and Mujica, L. E. "Damage Detection by Using FBGs and Strain Field Pattern Recognition Techniques." *Smart Materials and Structures*, Vol. 22, No. 2, 2012, p. 025011. https://doi.org/10.1088/0964-1726/22/2/025011.

[15] Ech-Choudany, Y., Assarar, M., Scida, D., Morain-Nicolier, F., and Bellach, B. "Unsupervised Clustering for Building a Learning Database of Acoustic Emission Signals to Identify Damage Mechanisms in Unidirectional Laminates." *Applied Acoustics*, Vol. 123, 2017, pp. 123–132. https://doi.org/10.1016/J.APACOUST.2017.03.008.

[16] Dia, A., Dieng, L., Gaillet, L., and Gning, P. B. "Damage Detection of a Hybrid Composite Laminate Aluminum/Glass under Quasi-Static and Fatigue Loadings by Acoustic Emission Technique." *Heliyon*, Vol. 5, No. 3, 2019, p. e01414. https://doi.org/10.1016/J.HELIYON.2019.E01414.

[17] Tiryaki, S., and Aydin, A. "An Artificial Neural Network Model for Predicting Compression Strength of Heat Treated Woods and Comparison with a Multiple Linear Regression Model." *Construction and Building Materials*, Vol. 62, 2014, pp. 102–108. https://doi.org/10.1016/J.CONBUILDMAT.2014.03.041.

[18] Gebraeel, N., Lawley, M., Liu, R., and Parmeshwaran, V. "Residual Life Predictions from Vibration-Based Degradation Signals: A Neural Network Approach." *IEEE Transactions on Industrial Electronics*, Vol. 51, No. 3, 2004, pp. 694–700. https://doi.org/10.1109/TIE.2004.824875.

[19] Banerjee, P., Palanisamy, R. P., Haq, M., Udpa, L., and Deng, Y. "Data-Driven Prognosis of Fatigue-Induced Delamination in Composites Using Optical and Acoustic NDE Methods." *2019 IEEE International Conference on Prognostics and Health Management, ICPHM 2019*, 2019. https://doi.org/10.1109/ICPHM.2019.8819426.

[20] Elenchezhian, M. R. P., Vadlamudi, V., Raihan, R. M., and Reifsnider, K. L. "Damage Precursor Identification in Composite Laminates Using Data Driven Approach." *AIAA Scitech 2019 Forum*, 2019. https://doi.org/10.2514/6.2019-0401.

[21] Elenchezhian, M. R. P., Vadlamudi, V., Raihan, R., Reifsnider, K., and Reifsnider, E. "Artificial Intelligence in Real-Time Diagnostics and Prognostics of Composite Materials and Its Uncertainties—a Review." *Smart Materials and Structures*, Vol. 30, No. 8, 2021, p. 083001. https://doi.org/10.1088/1361-665X/AC099F.

[22] Elenchezhian, M. R. P., Das, P. P., Rahman, M., Vadlamudi, V., Raihan, R., and Reifsnider, K. "Stiffness Degradation in Fatigue Life of Composites Using Dielectric State Variables." *Composite Structures*, Vol. 273, No. June, 2021, p. 114272. https://doi.org/10.1016/j.compstruct.2021.114272.

[23] Standard Test Method for Tension-Tension Fatigue of Polymer Matrix Composite Materials. https://www.astm.org/d3479_d3479m-12.html. Accessed May 13, 2022.

[24] Standard Test Method for Tensile Properties of Polymer Matrix Composite Materials. https://www.astm.org/d3039_d3039m-08.html. Accessed May 13, 2022.

[25] Hara, K., Saito, D., and Shouno, H. "Analysis of Function of Rectified Linear Unit Used in Deep Learning." *Proceedings of the International Joint Conference on Neural Networks*, Vols. 2015-September, 2015. https://doi.org/10.1109/IJCNN.2015.7280578.

[26] Kingma, D. P., and Lei Ba, J. "Adam: A Method for Stochastic Optimization." *undefined*, 2015.

[27] Saputro, D. R. S., and Widyaningsih, P. "Limited Memory Broyden-Fletcher-Goldfarb-Shanno (L-BFGS) Method for the Parameter Estimation on Geographically Weighted Ordinal Logistic Regression Model (GWOLR)." *AIP Conference Proceedings*, Vol. 1868, No. 1, 2017, p. 040009. https://doi.org/10.1063/1.4995124.